Simple and Sensitive Electrochemical Determination of L-Tryptophan at Electrochemically Activated Glassy Carbon Electrode

Diro, Abebe; Addisu Kitte, Shimeles*+; Feyisa, Tilahun Yai
Department of Chemistry, College of Natural Sciences, Jimma University, P. O. Box 378, Jimma, ETHIOPIA

Kelecha, Abiyot
Chemistry Department, Faculty of Natural and Computational Science, Mettu University, Mettu, ETHIOPIA

ABSTRACT: *Herein, we reported an Activated Glassy Carbon Electrode (AGCE) for the detection of L-tryptophan (Trp). AGCE was made by successive cyclic voltammetric potential scanning of glassy carbon electrode (GCE) from -1.5 V to 2.5 V in 0.1 M pH 7.0 phosphate buffer as a supporting electrolyte. The surface morphology of AGCE and Un-Activated Glassy Carbon Electrode (UGCE) was characterized by a Scanning Electron Microscope (SEM). The voltammetric sensing of Trp is carried out using Cyclic Voltammetry (CV) and Linear Sweep Voltammetry (LSV). The electrochemical properties of the AGCE and UGCE were also examined by CV and Electrochemical Impedance Spectroscopy (EIS). AGCE exhibited enhanced anodic peak current and less overpotential for the oxidation of Trp than UGCE. LSV was used for the quantitative determination of Trp. Two linear ranges were obtained for the determination of Trp using LSV from 2.5 μM – 20.0 μM and 2.0 μM – 100.0 μM. The limit of detection (3σ/m) was 0.098 μM. The current method was successfully used to detect Trp in urine and healthy human serum.*

KEYWORDS: *Electrochemical activation; activated glassy carbon electrode; L-tryptophan; linear sweep voltammetry.*

INTRODUCTION

L-tryptophan (Trp) is one of the essential amino acids that plays a vital role in human growth and metabolism [1]. It is an important part of hormones for neurotransmitters such as serotonin and other essential biomolecules in various biochemical routes. It has been widely applied for the control and cure of numerous illnesses. It is also crucial for keeping the balance of nitrogen in human nutrition [2-4]. Since the human body is unable to synthesize Trp, it is used as an additive in food and pharmaceuticals to avoid dietary insufficiencies [5]. Due to improper metabolization of Trp, highly harmful metabolites are formed and believed to be toxic to the human brain and cause schizophrenia, hallucinations, delusions, and can cause certain cancers [6-9]. Thus, it is of great importance to develop an accurate, consistent and cheap method to detect Trp in food, pharmaceutical and biological samples. So far, many analytical methods have been established for Trp sensing such as chromatographic [10,11], chemiluminescence [12,13], colorimetric [14] and electrochemical methods [15-18]. As Trp is electroactive,

* *To whom correspondence should be addressed.*
+ *E-mail: shimeles.addisu@ju.edu.et*
1021-9986/2023/6/ 1821-1831 11/$/6.01

electrochemical methods with high sensitivity, selectivity, fast response and easy operation gained more devotion. However, it is still difficult to assess Trp directly at unmodified electrodes due to the slowness of the redox process leads to high overpotential at the electrode [19].

Because of the fascinating properties, such as inexpensiveness, chemical stability, good electrical conductivity, high hardness, high electrochemical inertness, impermeability to gases, simplicity to surface modification and low thermal coefficient expansion, glassy carbon electrode (GCE) has become widely employed material as an electrode in electrochemical reaction [20-22]. In electrochemical reaction enhanced electron transfer process is highly needed for sensitive determination of electroactive species. Therefore, to have more electroactive surface and fast electrode kinetics, modification of electrode surface has gained considerable attention [23, 24]. In recent time the widely used approach for the modification of GCE is application of electrodeposition of conducting polymers [25], carbon containing materials [26], nanoparticles [27-31], organic monomers [32] and nanocomposite [33,34]. Due to the involvement of harmful materials and tiresome steps in the synthesis of nanomaterials and polymer, electrode surface modification with simple, convenient and low cost method is still highly needed [35]. Previous experimental works revealed that electrochemical activation of GCE takes place by applying high voltage to introduce surface functional groups which leads activation of its surface. Activation of electrode in electrochemical analysis is getting much consideration because of its simplicity, efficiency, sensitivity and low cost. The electrochemical activation process helps to obtain accurate, definite and reproducible electrochemical signals [36-38]. So electrochemically activated GCEs are demonstrating rapid electron transfer kinetic and low background current, better sensitivity, reversibility, reproducibility, stability and reduced over potential compared with their precursors [39-42].

Therefore, in this study the activated GCE (AGCE) was employed for sensitive electrochemical detection of Trp. The electrochemical response of Trp was studied at un-activated GCE (UGCE) and AGCE. The AGCE displays better electrochemical performance than the inactivated one. Hence, the AGCE has been used for the electrochemical investigations of Trp.

EXPERIMENTAL SECTION

Chemicals

Trp obtained from Sinopharm Chemical Reagent Co. Ltd. (Beijing, China), dopamine (DA) and uric acid (UA) purchased from Sigma–Aldrich (USA), potassium chloride (KCl), dipotassium hydrogen orthophosphate (K_2HPO_4) and potassium dihydrogen phosphate (KH_2PO_4) bought from Aladdin Bio-Chem technology (Shangai, China). All chemicals were used as received. Ultrapure water (18.25 MΩ cm) was used during the course of the experiments.

Instrumentations

Electrochemical impedance spectroscopy (EIS), cyclic voltammetry (CV) and linear sweep voltammetry (LSV) experiment was conducted with a CHI660 electrochemical workstation with three electrode system, using GCE, Ag/AgCl (saturated KCl) and platinum wire as a working, reference and auxiliary electrode, respectively. Surface morphology of UGCE and AGCE was measured with a scanning electron microscope (SEM) (Philips XL30 ESEM).

Preparation of AGCE

First of all GCE (3.0 diameter) was polished with slurry of alumina (0.3 and 0.05 µm sequentially) on a polishing pad and rinsed thoroughly with ultrapure water to obtain a clean electrode surface. Subsequently, the electrode was dipped in 0.1 M PBS (pH 7.0) and activated by scanning the potential between −1.5 and +2.5 V at 100 mV/s for 15 scans according to the literature procedure [43].

Sample preparation

The stock solution of Trp was prepared by dissolving an accurate mass and dissolved in appropriate volume of the solvent and stored in a refrigerator until used. Working solution of Trp was prepared by diluting appropriate volume of stock solution of Trp in 0.1 M PBS pH 4.0 at the day of the experiment. 0.1 M phosphate buffer solutions (PBS) pH 4.0 was prepared by mixing 0.1 M KH_2PO_4 and K_2HPO_4 each and used as supporting electrolyte throughout the experiments.

Real sample analysis

For real samples analysis, the percentage recoveries were done by spiking different standard solution of Trp

in 200 folds diluted healthy human urine and serum. 10.0 µL of the collected human serum and urine was diluted to 2000.0 µL in 0.1 M PBS pH 4.0. Then, 15 µM and 20 µM standard Trp was spiked into the diluted serum and urine samples followed by determination of Trp in the diluted and spiked samples.

RESULTS AND DISCUSSION

Activation of GCE

Figure 1A exhibits uninterrupted CVs of GCE in 0.1 M pH 7.0 PBS as a supporting electrolyte by potential scanning from -1.5 to 2.5 V. Anodic peak nearly at 1.5 V and the cathodic peak at about -0.65 V were observed, respectively at the first scan. In the consequent scanning, a new oxidation peak was found at +0.4 V, and then the value of the peak current increased with the continuous scanning. This indicates the anodization of the GCE at high potential possibly due to the introduction of different surface functional groups, and then undergo cathodic process [43]. After ten scans, the peak currents at 1.5 V and at -0.65 V almost remain constant, so ten scans were selected for the activation of the GCE.

CV and EIS characterization of the electrode

CV and EIS were used to examine the electrochemical activities of UGCE and AGCE in 5 mM $[Fe(CN)_6]^{3-/4-}$ containing 0.1 M KCl. As shown in Figure 1B, a pair of reversible redox peaks of $[Fe(CN)_6]^{3-/4-}$ was seen at both UGCE and AGCE. But AGCE exhibited enhanced redox peak current than UGCE. Using the Randles Sevcik equation, the active surface area of both electrodes was calculated from the CV peak current and the diffusion coefficient of $[Fe(CN)_6]^{3-}$ [44].

$$i_p = 2.69\times10^5 n^{3/2} A D^{1/2} v^{1/2} C$$

where n is the number of electrons involved (1 for $[Fe(CN)_6]^{3-}$), A the electrode surface area, D the diffusion coefficient (7.6×10^{-6} cm^2s^{-1}), the scan rate (0.1 Vs^{-1}), and C the concentration of $[Fe(CN)_6]^{3-}$ (5×10^{-3} $molcm^{-3}$). The active surface area of AGCE was obtained as 0.35 cm^2 whereas the UGCE was 0.016 cm^2. The active surface area of AGCE was about 2.19 times greater than UGCE.

EIS is also an important technique to examine the interfacial electrochemical behavior of an electrode. So the impedance of the UGCE and AGCE was studied by recording EIS data in the solution containing

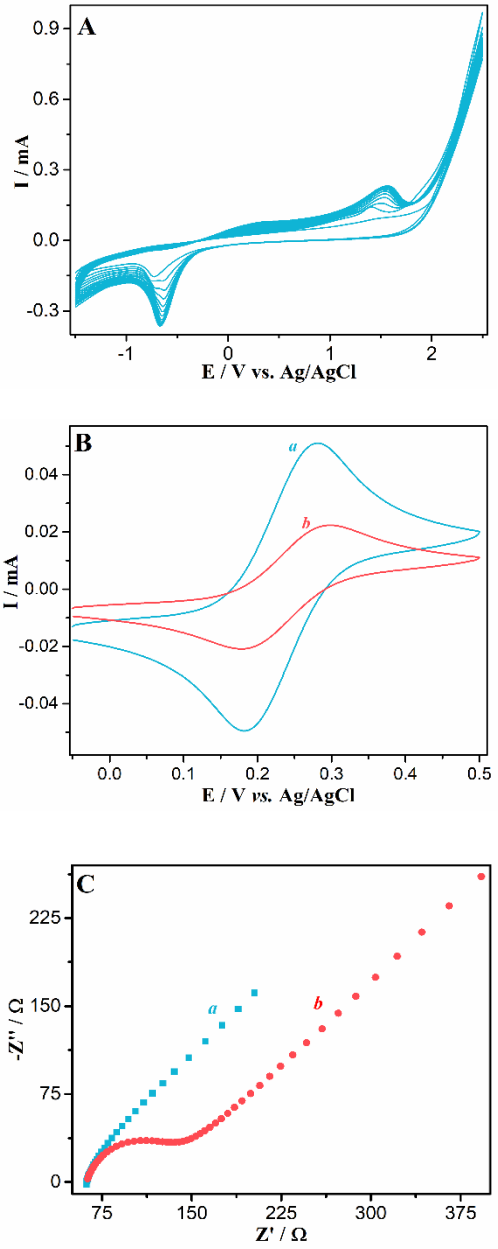

Fig. 1: (A) Continuous CVs (30 cycles) of GCE in 0.1 M pH 7.0 PBS; (B) and (C) CVs and the Nyquist plots of the UGCE (a) and AGCE (b) in 5 mM $[Fe(CN)_6]^{3-/4-}$ solution in 0.1 M KCl; scan rate 0.1 Vs^{-1}.

$[Fe(CN)6]^{3-/4-}$. The diameter of the semicircle of the Nyquist plots is equivalent to the charge transfer resistance (R_{ct}) at the electrode surface [45]. Figure 1C shows the R_{ct} of the AGCE (curve *a*) obtained was almost zero. Whereas, R_{ct} of UGCE (curve b) was about 150 Ω, indicating that the activation

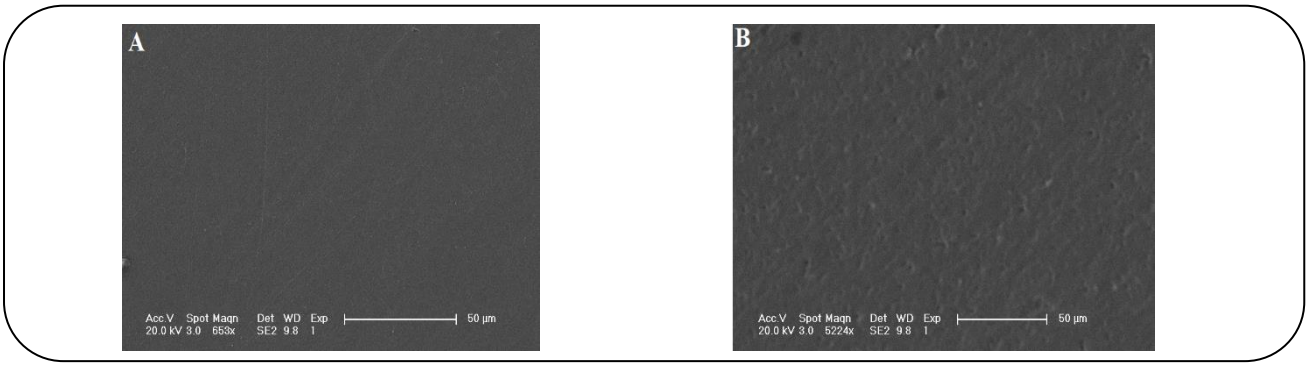

Fig. 2: SEM images of (A) UGCE and (B) AGCE.

of GCE remarkably improved the conductivity of the electrode.

Morphological analysis of UGCE and AGCE

Morphological investigation of UGCE and AGCE was done using SEM to study the changes that take place during the anodization of the GCE. As we can see from Figure 2, the AGCE shows a relatively rough surface (Figure 2A) as compared to UGCE (Figure 2B) which could be ascribed to activation of the GCE surface.

Electrochemical behavior of Trp at UGCE and AGCE

The CVs of 0.1 mM Trp at UGCE and AGCE in 0.1 M pH 4.0 PBS were shown in Figure 3A. It can be observed that the oxidation peak current and potential at the UGCE is about 0.015 mA and 1.0 V (Figure 3A curve *c*), respectively, while the anodic peak current response is noticeably enhanced at the AGCE (Figure 3A curve *d*), and the oxidation peak potential is shifted cathodically. AGCE gives an anodic peak potential and current at 0.93 V and 0.09 mA, respectively.

The experimental result shows the enhancement in the electrochemical response of Trp at the AGCE is about 6 times greater in the anodic peak current than the peak current at UGCE and nearly 70 mV of the oxidation peak potential shifts to the negative side. This can be ascribed to the introduction of more surface functional groups during activation and their catalytic role.

Effect of scan rate

The impact of the scan rate on the anodic peak current of Trp was examined at AGCE by CV method and shown in Figure 3B. The anodic peak currents of Trp rise with rising scan rate from 10 to 169 mV/s. Moreover, the peak currents of Trp is directly correlated to the square root of the scan rate (Figure 3C) in the studied scan rate range, which shows the anodic reaction of Trp was diffusion-controlled. To confirm the irreversibility of the anodic process of Trp at the AGCE, the correlation between the oxidation peak potential and scan rate was studied. It was seen that the anodic peak potential slowly shifted to more positive values on the rise in the scan rate. The correlation between the anodic potential (E) and the logarithm of scan rate (log v) was presented in Figure 3D. It is observed that E is linearly proportional to log v and the regression equation was found to be E (V) = 0.063 log v + 0.945 (R^2 = 0.988) in the scan rate range of 9 to 169 mV/s. According to Laviron's equation, the peak potential for an irreversible electrode reaction is given by equation [46]:

$$E = E^o + \left(\frac{2.303RT}{\alpha nF}\right)\log\left(\frac{RTk^o}{\alpha nF}\right) + \frac{2.303RT}{\alpha nF}\log v$$

Where α is the transfer coefficient, k^0 is the formal heterogeneous rate constant of the redox reaction, n is the number of electrons involved in the redox reaction, v is the scan rate, E^0 is the standard redox potential and the other symbols have their common meanings. Therefore, the value of αn can be obtained from the slope of E *vs* log v in the above equation.

In most systems, the value of α found between 0.3 and 0.7, and it can commonly be estimated by 0.5 in the absence of actual measurements [44]. Thus, the number of electrons transferred during the oxidation of Trp was calculated to be 1.9 ~ 2.0. According to the above results, the electrochemical reaction of tryptophan on AGCE was a two-electron two-proton process.

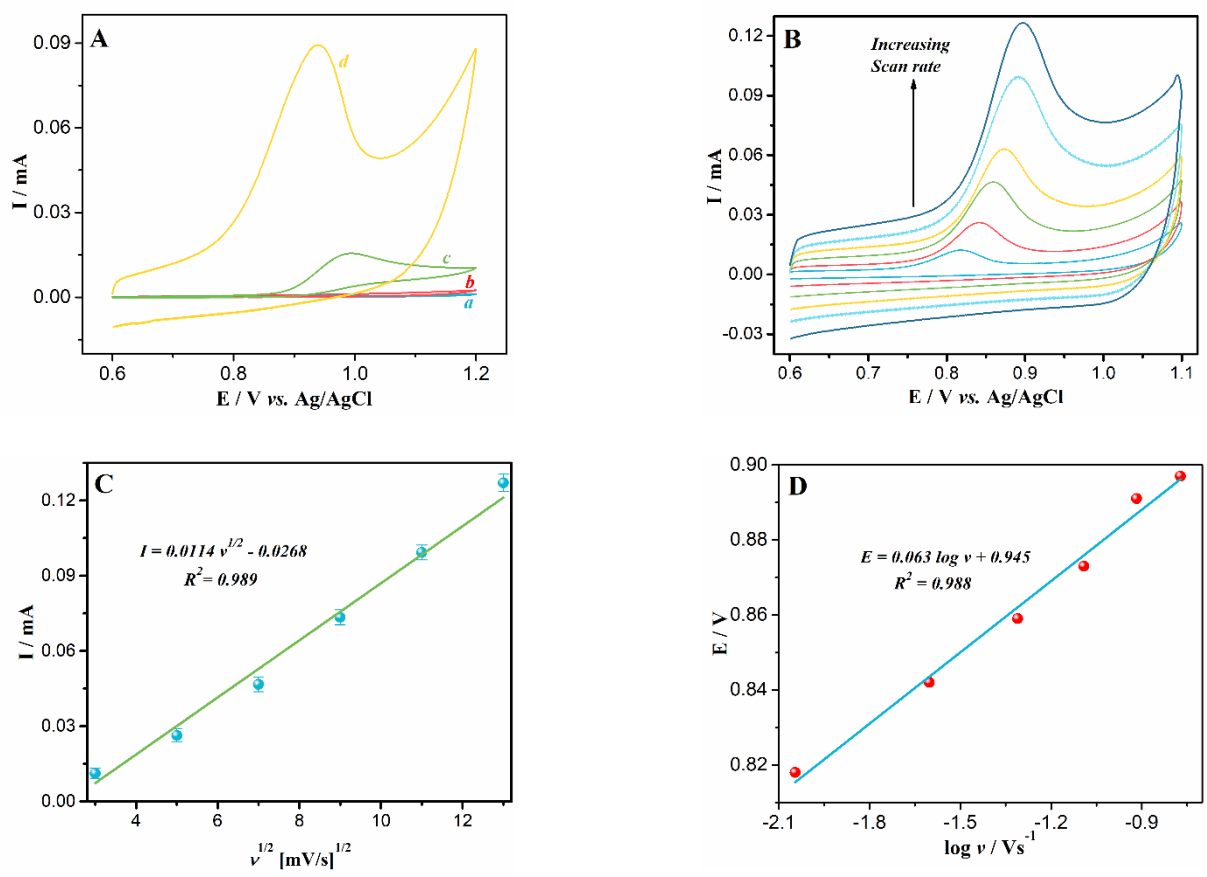

Fig. 3: (A) CVs recorded at UGCE in blank (PBS) (a) and with 0.1 mM Trp (c); AGCE in blank (PBS) (b) and with 0.1 mM Trp (d) in 0.1 M PBS pH 4; scan rate 0.1 Vs^{-1}; (B) CVs of 0.1 mM Trp recorded at AGCE in 0.1 M pH 4.0 PBS with different scan rates (9, 25, 49, 81, 121 and 169 mV/s); (C) Plot of I (mA) vs. $v^{1/2}$ [mV/s]; (D) Plot of E (V) vs. log v (V/s).

Effect of pH

The effect of the pH on the anodic peak currents and potentials of 0.1 mM Trp were studied by CV in the pH range of 2.0 to 8.0 at 100 mV/s. As represented in Figure 4A and B, the oxidation peak current increases when the pH increases from 2.0 to pH 4.0, and then declines with a further increase in pH. As a result, pH 4.0 was chosen as the optimum pH for the consequent experiments. Moreover, the anodic peak potential was also affected by a change in pH. The anodic peak potential of Trp shifted negatively with an increase in pH values (Figure 4B), indicating the involvement of the proton in the oxidation process. The anodic peak potential is directly related to pH with a calibration equation of E (V) = -0.049pH + 1.07, R^2 = 0.992. For pH *vs.* peak potential plot, the theoretical value for the slope is -0.059V/pH for the transfer of equal numbers of protons and electrons [47]. Here, the slope obtained is about 0.049V/pH, which is close to the theoretical value. Therefore, we can conclude that during the oxidation process of Trp of equal number of protons and electrons are involved as represented by Scheme 1. Trp is oxidized by a participation of two electron-two proton process takes place at the amine in the indole ring and methyl in the side chain.

Calibration curve

The electrochemical behaviors of Trp with different concentrations were studied using LSV under the optimum reaction conditions. The LSV experiment shows the anodic peak current (I_{pa}) increases with increasing concentration (Figure 5A). As shown in Figure 5B, the change of LSVs indicates that the oxidative peak current (I_{pa}) is correlated directly to the concentration (C) of Trp in two linear ranges between 2.5 µM and 20.0 µM and 20.0 µM and 100.0 µM, with a linear regression equations:

I_{pa} = 0.0034 C (µM) + 0.0091, R^2 = 0.993 and

I_{pa} = 0.0005 C (µM) + 0.0651, R^2 = 0.995, respectively.

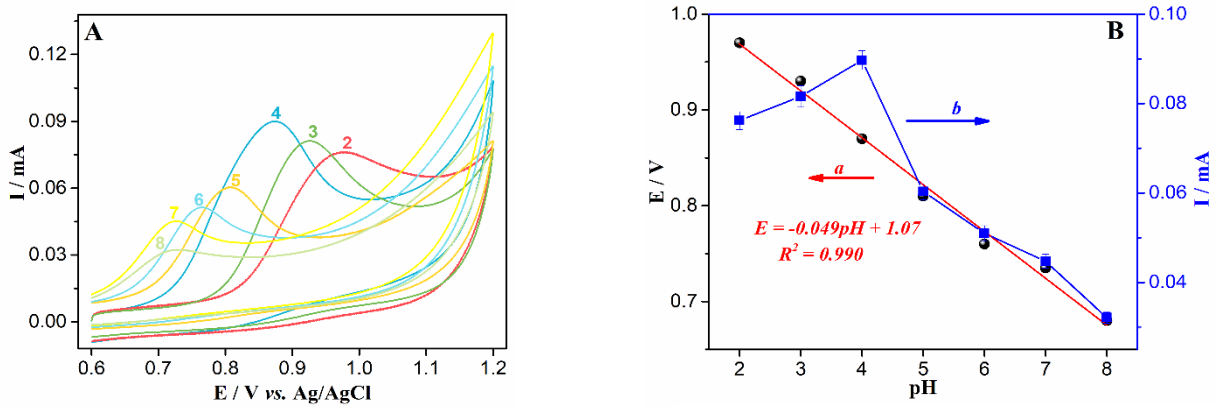

Fig. 4: (A) CVs at AGCE in buffer solutions containing 0.1 mM Trp of different pH; (B) Plot of variation of E and I of 0.1 mM Trp in buffer solutions of different pH at AGCE; (scan rate: 0.1 Vs^{-1}).

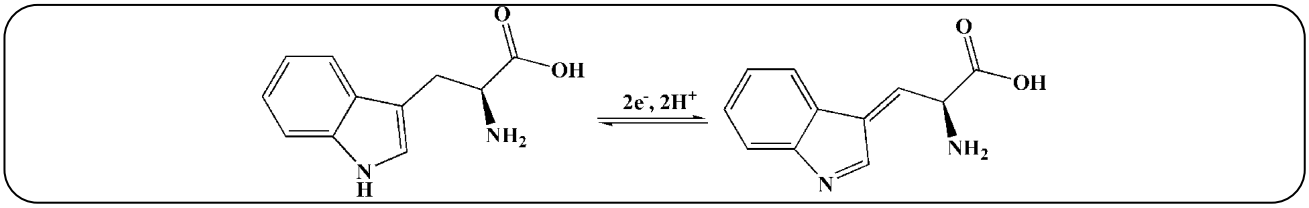

Scheme 1: Anodic reaction mechanism of Trp at AGCE.

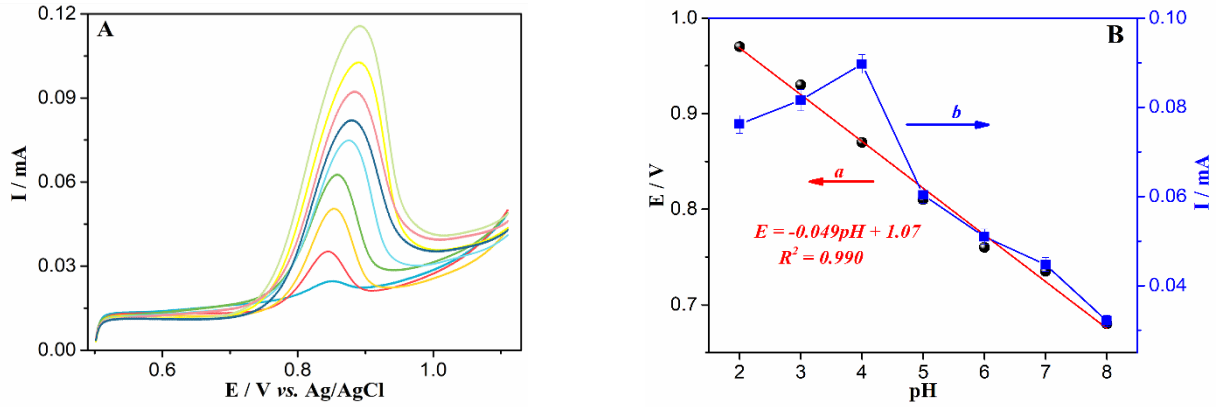

Figure 5. LSVs recorded (A) for determination of different concentration of Trp, (B) the calibration curve (plots of I_{pa} vs. C_{Trp}).

The obtained Limit of Detection (LOD) ($3\sigma/m$) was 0.92 µM. The dynamic linear range and LOD of the present work was compared with other related electrochemical techniques reported earlier in the literature for the detection of Trp and summarized in Table 1. We can confirm that the AGCE attained a comparable linear range and LOD with the previously reported electrochemical methods.

Repeatability and reproducibility

Fig. 6A shows the LSVs recorded ten times for 20 µM for the same electrode. The extent of repeatability shows outstanding precision of AGCE. Also, the Relative Standard Deviation (%***RSD***) of the oxidation peak currents obtained for ten measurements of 20 µM Trp at the same electrode was about 1.3% (n = 10). Similarly, the reproducibility of AGCE was evaluated by comparing the values of the oxidation current of Trp of three AGCEs independently activated under the same experimental conditions as shown in Figure 6B. The %*RSD* of the anodic current responses of 20 µM Trp was 3.87% (n = 3).

Table 1: Comparisons of the electrochemical performances of AGCE with other Trp sensors.

Electrode materials	Technique	Linear range (µM)	LOD (µM)	Ref
AuNPs/Polyimidazole/GCE	DPV	3.0 - 34.0 and 84.0 - 464.0	0.7	[48]
Clay-ZnHCF/CPE	SWV	2.4 - 24.0 and 24.0 - 60.0	0.8	[49]
Au NPs/ Carbon Ionic Liquid Electrode	SWV	5.0 - 900.0	4	[50]
Nafion/TiO_2-graphene/GCE	DPV	5.0 - 140.0	0.7	[51]
β-CD/carbon QDs/GCE	DPV	5.0 - 270.0	0.16	[52]
Fe_3O_4/C/GCE	LSV	1.0 - 80.0 and 80.0 - 800.0	0.26	[53]
AGCE	LSV	2.5 – 20.0 and 20.0 – 100.0	0.92	This work

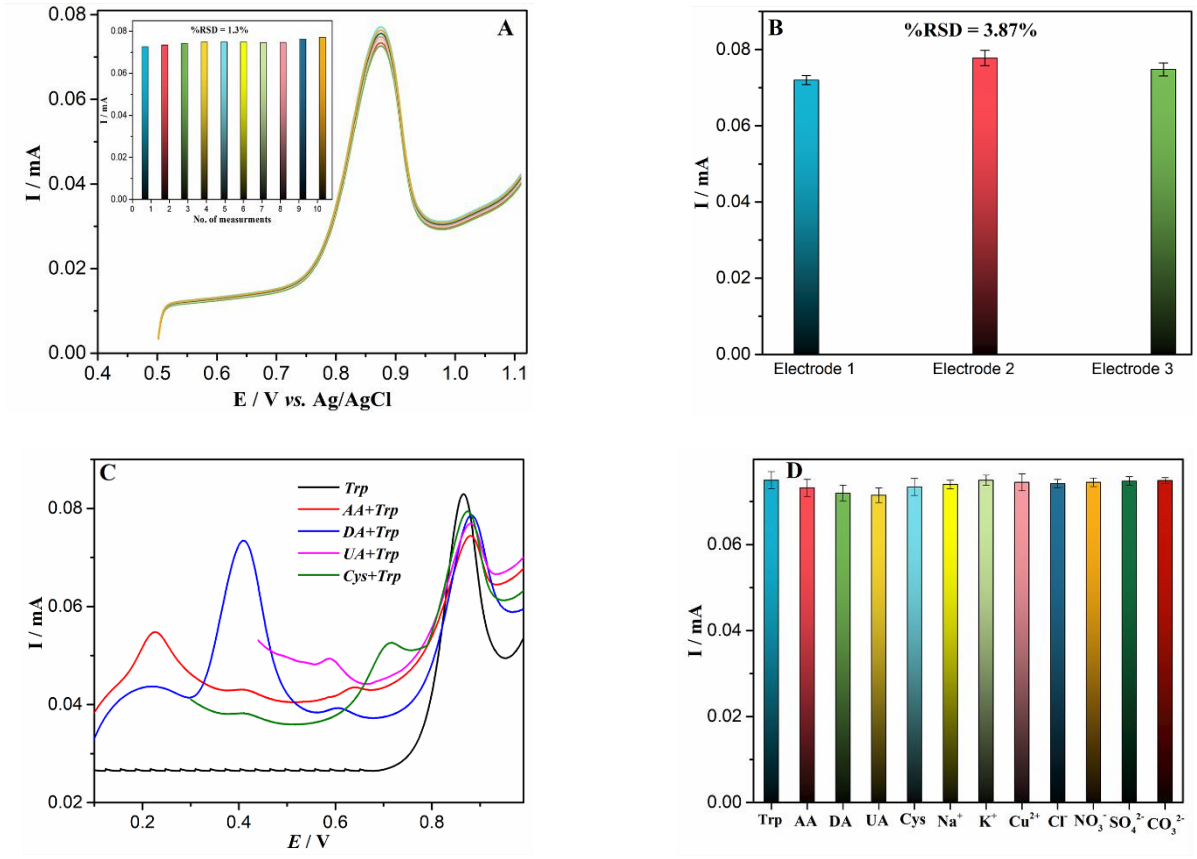

Fig. 6: (A) LSV recorded for 10 successive measurement of 20 µM Trp at AGCE in 0.1 M pH 4.0 PBS (Inset: Bar graph showing the current value for each measurement); (B) Comparison for the reproducibility of three electrodes separately activated; (C) LSV of Trp and mixture of AA, DA, UA and Cys (D) Effect of Interferences.

Real sample analysis

To examine the analytical application of AGCE for real samples, recovery experiments were done by standard addition method. 15.0 µM and 20.0 µM standard Trp were spiked into 200 times diluted healthy human serum and urine (Figure 7). As revealed in Table 2, using AGCE the detection of Trp found satisfactory recoveries from 92.0−109.3%. Therefore, it is a good candidate for the practical detection of Trp in biological samples.

Effect of interferences

For the selectivity of the method, interferences that might coexist in biological fluids were tested and the result is shown in Figure 6C and Figure 6D. The oxidation

Table 2: Real sample analysis results for Trp detection in healthy human serum and urine samples.

Sample	Added (µM)	Found (µM)	RSD,%	Recovery, %
Serum	15.0	15.84	1.75	94.7
	20.0	18.8	1.55	109.3
Urine	15.0	15.26	2.02	98.3
	20.0	21.74	1.52	92.0

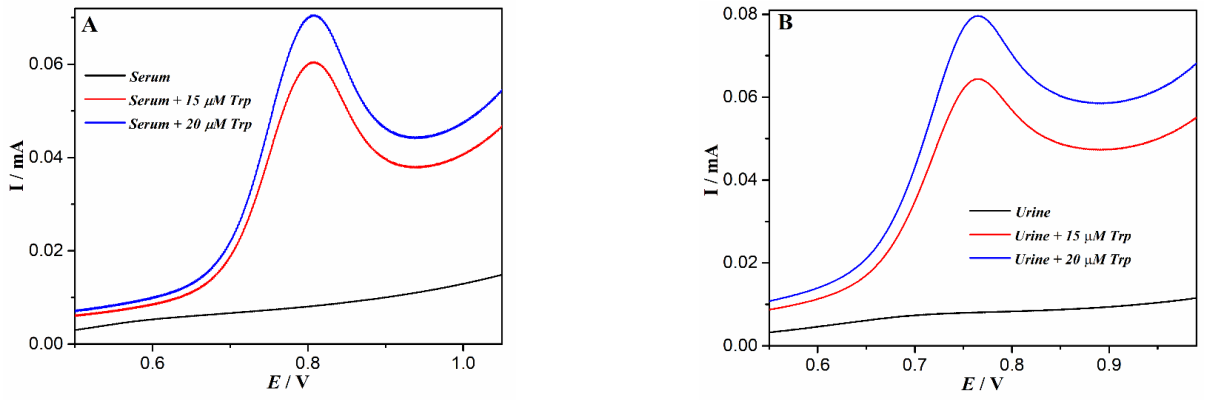

Fig. 7: LSV of determination of Trp in serum (A) and urine (B).

current of 20 µM of Trp with 100 fold excess of common ions for instance Na^+, K^+, Cu^{2+}, Cl^-, NO_3^-, CO_3^{2-}, and SO_4^{2-} did not show interference for Trp detection. Also 10-fold concentrations of commonly found substances in biological samples such as ascorbic acid, dopamine, uric acid and cysteine had less than 5% interfering effect. This suggests good selectivity of AGCE for the detection of Trp.

CONCLUSIONS

To sum up, GCE was activated by electrochemical method in PBS as a supporting electrolyte by potential scanning from -1.5 to 2.5 V. Due to the introduction of different functional groups on the surface of GCE, the AGCE owns high effective surface area and different functional groups, which is very beneficial for electrochemical sensing application. Hence, the performance of the AGCE is better than UGCE. The analytical performance of the AGCE was examined using CV and LSV for the detection of Trp. AGCE exhibited outstanding catalytic activity towards the oxidation of Trp and revealed a low detection limit. Moreover, ACGE was successfully employed for the detection of Trp in healthy human serum and urine.

Received : Jul. 2, 2022 ; Accepted : Oct. 10,2022

REFERENCES

[1] Zhu D., Bai Z., Ma H., Tan L., Pang H., Wang X., High Performance Simultaneous Detection of β-Nicotinamide Adenine Dinucleotide and L-Tryptophan in Human Serum Based on a Novel Nanocomposite of Ferroferric Oxide-Functionalized Polyoxometalates, *Sensor. Actuat. B: Chem.*, **309**: 127787 (2020).

[2] Ba X., Luo L., Ding Y., Liu X., Determination of L-Tryptophan in the Presence of Ascorbic Acid and Dopamine Using Poly(Sulfosalicylic Acid) Modified Glassy Carbon Electrode, *Sensor. Actuat. B: Chem.*, **187**: 27-32 (2013).

[3] Keyvanfard M., Shakeri R., Karimi-Maleh H., Alizad K., Highly Selective and Sensitive Voltammetric Sensor Based on Modified Multiwall Carbon Nanotube Paste Electrode for Simultaneous Determination of Ascorbic Acid, Acetaminophen and Tryptophan, *Mater. Sci. Eng.: C*, **33**: 811-816 (2013).

[4] Haldorai Y., Yeon S.-H., Huh Y. S., Han,Y.-K., Electrochemical Determination of Tryptophan Using a Glassy Carbon Electrode Modified with Flower-Like Structured Nanocomposite Consisting of Reduced Graphene Oxide and SnO_2. *Sensor. Actuat. B: Chem.*, **239:** 1221-1230 (2017).

[5] Baytak A.K., Aslanoglu M., Voltammetric Quantification of Tryptophan Using a MWCNT Modified GCE Decorated with Electrochemically Produced Nanoparticles of Nickel, *Sensor. Actuat. B: Chem.*, **220**: 1161-1168 (2015).

[6] Li J., Jiang J., Xu Z., Liu M., Tang S., Yang C., Qian D., Facile synthesis of Pd−Cu@Cu_2O/N-RGO Hybrid and its Application for Electrochemical Detection of Tryptophan, *Electrochim. Acta*, **260**: 526-535 (2018).

[7] Lian W., Ma D. J., Xu X., Chen Y., Wu Y. L., Rapid High-Performance Liquid Chromatography Method For Determination of Tryptophan in Gastric Juice, *J. Dig. Dis.*, **13**: 100-106 (2012).

[8] Kumar J. V., Karthik R., Chen S.-M., Marikkani S., Elangovan A., Muthuraj V., Green Synthesis of a Novel Flower-Like Cerium Vanadate Microstructure for Electrochemical Detection of Tryptophan in Food and Biological Samples, *J. Colloid Interface Sci.*, **496**: 78-86 (2017).

[9] Wang L., Yang R., Li J., Qu L., Harrington P.d.B., A Highly Selective and Sensitive Electrochemical Sensor for Tryptophan Based on the Excellent Surface Adsorption and Electrochemical Properties of PSS Functionalized Graphene, *Talanta*, **196**: 309-316 (2019).

[10] Zhang L., Li Y., Zhou H., Li L., Wang Y., Zhang, Y., Determination of Eight Amino Acids in Mice Embryonic Stem Cells by Pre-Column Derivatization HPLC with Fluorescence Detection, *J. Pharm. Biomed. Anal.*, **66**: 356-358 (2012).

[11] Dario M.F., Freire T.B., Pinto C.A., Prado M.S., Baby A.R., Velasco M.V., Tryptophan and Kynurenine Determination in Human Hair by Liquid Chromatography. *J. Chromatogr. B*, **1065-1066**: 59-62 (2017).

[12] Qiu H., Luo C., Sun M., Lu F., Fan L., Li X., Determination of L-Tryptophan Based on Graphene Oxide–Magnetite-Molecularly Imprinted Polymers and Chemiluminescence, *Talanta*, **98**: 226-230 (2012).

[13] Lin Z., Chen X., Cai Z., Li P., Chen X., Wang X., Chemiluminescence of Tryptophan and Histidine in $Ru(bpy)_3^{2+}$-$KMnO_4$ Aqueous Solution, *Talanta*, **75**: 544-550 (2008).

[14] Li H., Li F., Han C., Cui Z., Xie G., Zhang A., Highly Sensitive and Selective Tryptophan Colorimetric Sensor Based on 4,4-Bipyridine-Functionalized Silver Nanoparticles, *Sensor. Actuat. B: Chem.*, **145:** 194-199 (2010).

[15] Özcan A., Şahin Y., A Novel Approach for the Selective Determination of Tryptophan in Blood Serum in the Presence of Tyrosine Based on the Electrochemical Reduction of Oxidation Product of Tryptophan Formed in Situ on Graphite Electrode, *Biosens. Bioelectron.*, **31**: 26-31 (2012).

[16] Jin G.-P., Lin X.-Q., The Electrochemical Behavior and Amperometric Determination of Tyrosine and Tryptophan at a Glassy Carbon Electrode Modified With Butyrylcholine, *Electrochem. Commun.*, **6**: 454-460 (2004).

[17] Han J., Zhao J., Li Z., Zhang H., Yan Y., Cao D., Wang G., Nanoporous Carbon Derived From Dandelion Pappus as an Enhanced Electrode Material with Low Cost for Amperometric Detection of Tryptophan, *J. Electroanal. Chem.*, **818**: 149-156 (2018).

[18] Liu B., Ouyang X., Ding Y., Luo L., Xu D. Ning Y., Electrochemical Preparation of Nickel and Copper Oxides-Decorated Graphene Composite for Simultaneous Determination of Dopamine, Acetaminophen and Tryptophan, *Talanta*, **146**: 114-121 (2016).

[19] Gautam J., Raj M., Goyal R. N., Determination of Tryptophan at Carbon Nanomaterials Modified Glassy Carbon Sensors: A Comparison, *J. Electrochem. Soc.*, **167**: 066504 (2020).

[20] Dekanski A., Stevanović J., Stevanović R., Nikolić B.Ž., Jovanović V.M., Glassy carbon Electrodes: I. Characterization and Electrochemical Activation. *Carbon*, **39**: 1195-1205 (2001).

[21] Van der Linden W. E., Dieker J. W., Glassy Carbon as Electrode Material in Electro-Analytical Chemistry, *Anal. Chim. Acta*, **119**: 1-24 (1980).

[22] Bystron T., Sramkova E., Dvorak F., Bouzek K., Glassy Carbon Electrode Activation – A Way Towards Highly Active, Reproducible And Stable Electrode Surface, *Electrochim. Acta*, **299**: 963-970 (2019).

[23] Altuner E.E., Ozalp V.C., Yilmaz M.D., Sudagidan M., Aygun A., Acar E.E., Tasbasi B.B., Sen F., Development of Electrochemical Aptasensors Detecting Phosphate Ions on TMB Substrate with Epoxy-Based Mesoporous Silica Nanoparticles, *Chemosphere*, **297**: 134077 (2022).

[24] Altuner E.E., Ozalp V.C., Yilmaz M.D., Bekmezci M., Sen F., High-Efficiency Application of CTS-Co NPs Mimicking Peroxidase Enzyme on TMB(ox). *Chemosphere*, **292**: 133429 (2022).

[25] Biallozor S., Kupniewska A., Conducting Polymers Electrodeposited on Active Metals, *Synth. Met.*, **155**: 443-449 (2005).

[26] Shahrokhian S., Naderi L., Ghalkhani M., Modified Glassy Carbon Electrodes Based on Carbon Nanostructures for Ultrasensitive Electrochemical Determination of Furazolidone, *Mater. Sci. Eng. C.*, **61**: 842-850 (2016).

[27] Chang G., Shu H., Ji K., Oyama M., Liu X., He Y., Gold Nanoparticles Directly Modified Glassy Carbon Electrode for Non-Enzymatic Detection of Glucose, *Appl. Surf. Sci.*, **288**: 524-529 (2014).

[28] Ghoreishi S. M., Behpour M., Saeidinejad F., Electrochemical Determination of Tryptophan, Uric Acid and Ascorbic Acid at a Gold Nanoparticles Modified Carbon Paste Electrode, *Anal. Methods*, **4:** 2447-2453 (2012).

[29] Jandaghi N., Jahani S., Foroughi M. M., Kazemipour M., Ansari M., Cerium-Doped Flower-Shaped ZnO Nano-Crystallites as a Sensing Component for Simultaneous Electrochemical Determination of Epirubicin and Methotrexate, *Microchim. Acta*, **187**: 24 (2019).

[30] Foroughi, M. M.; Jahani, S., Investigation of a High-Sensitive Electrochemical DNA Biosensor for Determination of Idarubicin and Studies of DNA-Binding Properties, *Microchem. J.*, **179**: 107546 (2022).

[31] Foroughi M. M., Jahani S., Aramesh-Boroujeni Z., Rostaminasab Dolatabad M., Shahbazkhani K., Synthesis of 3D Cubic of Eu^{3+}/Cu_2O with Clover-Like Faces Nanostructures and their Application as an Electrochemical Sensor for Determination of Antiretroviral Drug Nevirapine, *Ceram. Int.*, **47**: 19727-19736 (2021).

[32] Jin G., Zhang Y., Cheng W., Poly(P-Aminobenzene Sulfonic Acid)-Modified Glassy Carbon Electrode for Simultaneous Detection of Dopamine and Ascorbic Acid, *Sens. Actuators B Chem.*, **107**: 528-534 (2005).

[33] Karimi-Maleh H., Moazampour M., Ahmar H., Beitollahi H., Ensafi A.A., A Sensitive Nanocomposite-Based Electrochemical Sensor for Voltammetric Simultaneous Determination of Isoproterenol, Acetaminophen and Tryptophan, *Measurement*, **51**: 91-99 (2014).

[34] Setoudeh N., Jahani S., Kazemipour M., Foroughi M.M., Hassani Nadiki H., Zeolitic Imidazolate Frameworks and Cobalt-Tannic Acid Nanocomposite Modified Carbon Paste Electrode for Simultaneous Determination of Dopamine, Uric Acid, Acetaminophen and Tryptophan: Investigation of Kinetic Parameters of Surface Electrode and its Analytical Performance, *J. Electroanal. Chem.*, **863**: 114045 (2020).

[35] Tilahun Yai F., Shimeles Addisu K., Dereje Y., Gebru G., Simultaneous Electrochemical Determination of Paracetamol and Caffeine using Activated Glassy Carbon Electrode, *Anal. Bioanal. Electrochem.*, **12**: 93-106 (2020).

[36] Sunil Kumar Naik T. S., Kumara Swamy B. E., Pre-Treated Glassy Carbon Electrode Sensor for Catechol: A Voltammetric Study, *J. Electroanal. Chem.*, **826**: 23-28 (2018).

[37] Mahanthesha K.R., Kumara Swamy B.E., Pretreated/Carbon Paste Electrode Based Voltammetric Sensors for the Detection of Dopamine in Presence of Ascorbic Acid and Uric Acid, *J. Electroanal. Chem.*, **703:** 1-8 (2013).

[38] Hailemichael A., Lebohang H., Voltammetric Determination of Chloramphenicol at Electrochemically Pretreated Glassy Carbon Electrode, *Bull. Chem. Soc. Ethiop.*, **21**: 1-12 (2007).

[39] Rana A., Baig N., Saleh T. A., Electrochemically Pretreated Carbon Electrodes and their Electroanalytical Applications – A Review, *J. Electroanal. Chem.*, **833**: 313-332 (2019).

[40] Qiao J. X., Luo H. Q., Li N. B., Electrochemical Behavior of Uric Acid and Epinephrine at an Electrochemically Activated Glassy Carbon Electrode, *Colloid. Surface B.*, **62**: 31-35 (2008).

[41] Hadi M., Rouhollahi A., Yousefi M., Taidy F., Malekfar R., Electrochemical Characterization of a Pyrolytic Carbon Film Electrode and the Effect of Anodization. *Electroanalysis*, **18**: 787-792 (2006).

[42] Nagaoka T., Fukunaga, T., Yoshino T., Watanabe I., Nakayama T., Okazaki S., Uptake of Ions by Electrochemically Treated Glassy Carbon. *Anal. Chem.*, **60**: 2766-2769 (1988).

[43] Abdel-Aziz A.M., Hassan H.H., Badr I.H.A., Glassy Carbon Electrode Electromodification in the Presence of Organic Monomers: Electropolymerization versus Activation, *Anal. Chem.*, **92:** 7947-7954 (2020).

[44] Allen J. Bard, Faulkner L. R., "Electrochemical Methods: Fundamentals and Applications". 2nd ed.; John Wiley & Sons, Inc (2000).

[45] Chang B.-Y., Park S.-M., Electrochemical Impedance Spectroscopy, *Annu. Rev. Anal. Chem.***, 3:** 207-229 (2010).

[46] Laviron E., General Expression of the Linear Potential Sweep Voltammogram in the Case of Diffusionless Electrochemical Systems, *J. Electroanal. Chem.*, **101**: 19-28 (1979).

[47] Frith K.A., Limson J.L., pH tuning of Nafion® for Selective Detection of Tryptophan, *Electrochim. Acta*, **54**: 3600-3605 (2009).

[48] Wang C., Yuan R., Chai Y., Chen S., Hu F., Zhang M., Simultaneous Determination of Ascorbic Acid, Dopamine, Uric Acid and Tryptophan on Gold Nanoparticles/Overoxidized-Polyimidazole Composite Modified Glassy Carbon Electrode, *Anal. Chim. Acta*, **741**: 15-20 (2012).

[49] Kemmegne-Mbouguen J. C., Angnes L., Mouafo-Tchinda E., Ngameni E., Electrochemical Determination of Uric Acid, Dopamine and Tryptophan at Zinc Hexacyanoferrate Clay Modified Electrode. *Electroanalysis*, **27**: 2387-2398 (2015).

[50] Safavi A., Momeni S., Electrocatalytic Oxidation of Tryptophan at Gold Nanoparticle-Modified Carbon Ionic Liquid Electrode, *Electroanalysis***, 22:** 2848-2855 (2010).

[51] Fan Y., Liu J.-H., Lu H.-T., Zhang Q., Electrochemistry and Voltammetric Determination of L-Tryptophan and L-Tyrosine Using a Glassy Carbon Electrode Modified with a Nafion/TiO_2-Graphene Composite Film, *Microchim. Acta*, **173**: 241-247 (2011).

[52] Chen J., He P., Bai H., He S., Zhang T., Zhang X., Dong F., Poly(β-cyclodextrin)/Carbon Quantum Dots Modified Glassy Carbon Electrode: Preparation, Characterization and Simultaneous Electrochemical Determination of Dopamine, Uric Acid and Tryptophan, *Sensor. Actuat. B: Chem.*, **252**: 9-16 (2017).

[53] Liu J., Dong S., He Q., Yang S., Xie M., Deng P., Xia Y., Li G., Facile Preparation of Fe_3O_4/C Nanocomposite and Its Application for Cost-Effective and Sensitive Detection of Tryptophan, *Biomolecules*, **9**: 245 (2019).